Available online at www.sciencedirect.com
ScienceDirect
Polymer 48 (2007) 3607–3611
polymer
www.elsevier.com/locate/polymer

Polymer Communication

Composition dependence of crystallized lamellar morphology formed in crystalline–crystalline diblock copolymers

Shuichi Nojima*, Keisuke Ito, Hiroshi Ikeda

Department of Organic and Polymeric Materials, Graduate School of Science and Engineering, Tokyo Institute of Technology, H-125, 2-12-1 Ookayama, Meguro-Ku, Tokyo 152-8552, Japan

Received 28 December 2006; received in revised form 2 April 2007; accepted 21 April 2007
Available online 4 May 2007

Abstract

We have investigated the crystallized morphology formed at each temperature T_c (20 °C $\leq T_c \leq$ 45 °C) in double crystalline poly(ε-caprolactone)-*block*-polyethylene (PCL-*b*-PE) copolymers as a function of composition (or volume fraction of PE blocks ϕ_{PE}) by employing small-angle X-ray scattering (SAXS) and differential scanning calorimetry (DSC) techniques. When PCL-*b*-PE with $\phi_{PE} \leq 0.58$ was quenched from a microphase-separated melt into T_c, the crystallization of PE blocks occurred first to yield an alternating structure consisting of thin PE crystals and amorphous PE + PCL layers (PE lamellar morphology) followed by the crystallization of PCL blocks, where we can expect a competition between the stability of the PE lamellar morphology (depending on ϕ_{PE}) and PCL crystallization (on T_c). Two different morphologies were formed in the system judging from a long period. That is, the PCL block crystallized within the existing PE lamellar morphology at lower T_c (<30 °C) to yield a double crystallized alternating structure while it crystallized by deforming or partially destroying the PE lamellar morphology at higher T_c (>35 °C) to result in a significant increase of the long period. However, the temperature at which the morphology changed was almost independent of ϕ_{PE}. For PCL-*b*-PE with $\phi_{PE} \geq 0.73$, on the other hand, the morphology after the crystallization of PE blocks was preserved at every T_c investigated.

Keywords: Crystalline–crystalline diblock copolymer; Composition; Lamellar morphology

1. Introduction

When crystalline–crystalline diblock copolymers are quenched from a microphase-separated melt into low temperatures, two different blocks are allowed to crystallize resulting in a complicated morphology in the system, which is mainly controlled by the molecular characteristics, in particular, melting temperature T_m of constituent blocks. If T_m values of both blocks are close enough, we expect a simultaneous crystallization of two blocks. Several experimental results are reported on the crystallization behavior and resulting morphology for di- and tri-block copolymers consisting of poly(ε-caprolactone) (PCL) and poly(ethylene oxide) [1–8], where T_m of both blocks is *ca.* 60 °C. On the other hand, T_m of one block is sufficiently higher than that of the other, the crystallization of high-T_m blocks occurs first to form a crystallized morphology followed by the crystallization of low-T_m blocks. The crystallization in this case is also reported for several double crystalline diblock copolymers with significantly different melting temperatures [9–19].

We have previously investigated the crystallization behavior and resulting morphology of low molecular weight PCL-*block*-polyethylene (PCL-*b*-PE) diblock copolymers [14,15], where T_m of PE blocks was *ca.* 100 °C and that of PCL blocks was *ca.* 60 °C, so that the PE block crystallized first during quenching to form an alternating structure consisting of thin PE crystals and amorphous PE + PCL layers (PE lamellar morphology), and subsequently the PCL block started to crystallize from this PE lamellar morphology. We found from these studies that the crystallization temperature T_c of PCL

* Corresponding author. Tel.: +81 3 5734 2132; fax: +81 3 5734 2888.
E-mail address: snojima@polymer.titech.ac.jp (S. Nojima).

0032-3861/$ - see front matter © 2007 Elsevier Ltd. All rights reserved.
doi:10.1016/j.polymer.2007.04.053

blocks intimately affected the crystallization behavior and eventually resulting morphology. That is, at lower T_c (<30 °C), the PE lamellar morphology was completely preserved and consequently PCL blocks crystallized within this lamellar morphology as a template. At higher T_c (>35 °C), on the other hand, the PCL block crystallized by deforming and/or partially destroying the existing PE lamellar morphology to yield a new lamellar morphology favorable for the crystallization of PCL blocks (see Fig. 7 of Ref. [14]).

The experimental facts mentioned above indicate that the PE lamellar morphology works as a *spatial confinement* against PCL crystallization, which is qualitatively similar to a molten microdomain for the crystallization of constituent blocks in crystalline–amorphous diblock copolymers [20–23], where the total molecular weight of block copolymers mainly controls the stability of microdomains. Therefore it is necessary to investigate the stability of the PE lamellar morphology against PCL crystallization for better understanding of the morphology formed in PCL-*b*-PE. We expect intuitively that the stability of the PE lamellar morphology can be changed with changing the volume fraction of PE blocks ϕ_{PE} or the crystallinity of PE blocks in the whole system χ_{PE}; when χ_{PE} increases the stability will increase accordingly. This is the motivation of this study, and we investigate the morphology finally formed in PCL-*b*-PE with different compositions, and summarize the results as a function of χ_{PE}.

2. Experimental

2.1. Samples

PCL-*b*-PE copolymers were obtained by the hydrogenation of PCL-*block*-polybutadiene (PCL-*b*-PB) diblocks anionically synthesized under vacuum. The method of PCL-*b*-PB synthesis and hydrogenation was described elsewhere [14,15,24]. The molecular characteristics of PCL-*b*-PE used in this study are shown in Table 1, where the three copolymers (denoted by A1, A2, and A3) were already used in our previous studies [14,15]. The total molecular weight is less than 18,000 for all copolymers, so that the morphological transition from a microdomain structure into the PE lamellar morphology is expected when PCL-*b*-PE is quenched into low temperatures (<45 °C). Actually the transition was confirmed for E25, E31, E36, E49, and E58 by the temperature dependence of the long period, by which Quiram et al. [25] first demonstrated the morphological transition in PE-based crystalline–amorphous diblocks. This means that the type of microdomain structures does not affect the crystallization behavior of PCL blocks and resulting morphology because they disappear completely instead the PE lamellar morphology prevails in the system when PCL blocks start to crystallize. For E86 and E73, on the other hand, the morphological transition was not confirmed; the PE blocks might crystallize within the molten microdomains (confined crystallization). However, the PE lamellar morphology is finally formed in these copolymers because the PE block is a major component (or matrix), though the state of the amorphous PCL phase is slightly different. As a result, the volume fraction of PE blocks in PCL-*b*-PE ϕ_{PE} changes from 0.86 to 0.25, and we can expect a wide variation in χ_{PE} leading to a large change in the stability of the PE lamellar morphology against PCL crystallization.

Table 1
Molecular characteristic of PCL-*b*-PE copolymers used in this study

	M_n[a]	M_w/M_n[b]	PCL:PE[c] (vol.%)	EB[c] (mol%)	$T_{m,PCL}$[d] (°C)	$T_{m,PE}$[d] (°C)
E86	14,000	1.16	14:86	–	50	103
E73	16,000	1.13	27:73	–	55	102
E58 (A1)	8400	1.13	42:58	6	58	101
E49 (A3)	18,000	1.18	51:49	5	59	100
E36	13,000	1.16	64:36	7	59	97
E31 (A2)	11,000	1.09	69:31	6	59	99
E25	14,000	1.08	75:25	–	59	101

[a] Determined by membrane osmometry.
[b] Determined by GPC.
[c] Determined by ^{1}H NMR (EB: ethyl branch).
[d] Determined by DSC for the samples crystallized at 0 °C for 10 min.

2.2. Differential scanning calorimetric (DSC) measurements

A Perkin–Elmer DSC Pyris 1 was used to evaluate χ_{PE} just before the crystallization of PCL blocks. The sample was cooled with a rate of 10 °C/min from a microphase-separated melt at 120 °C down to 0 °C, where the crystallization of PCL blocks finished completely. χ_{PE} was calculated from the exothermic peak area located at *ca*. 85 °C (see Fig. 1a) by assuming that the exothermic heat to form perfect PE crystals was 277 J/g [26]. χ_{PE} is almost equal to the volume fraction of PE crystals existing in the system, so that it will be a direct measure rather than ϕ_{PE} for the stability of the PE lamellar morphology against PCL crystallization.

2.3. Small-angle X-ray scattering (SAXS) measurements

The microphase-separated sample at 130 °C was rapidly quenched into each T_c and annealed there for a long time (from 30 min to 3 days depending on T_c), where the long period did not change at all during annealing though it depended significantly on T_c. The PE block crystallized rapidly during quenching, so that the PCL block started to crystallize from the crystallized PE morphology at every T_c. The resulting morphology was investigated mainly by synchrotron SAXS (SR-SAXS) and complementally by conventional SAXS. The results obtained by two techniques coincided with each other and no systematical error could be detected.

SR-SAXS measurements were performed using synchrotron radiation at Photon Factory in High-energy Accelerator Research Organization, Tsukuba, Japan, with a small-angle X-ray equipment for solution installed at beam line BL-10C. Details of the equipment and the intensity correction procedure were already described elsewhere [24,27]. The SAXS curves were finally obtained as a function of $s = (2/\lambda)\sin\theta$, where λ is the wavelength of incident X-ray (=0.1488 nm) and 2θ is the scattering angle. In this study, we focused our

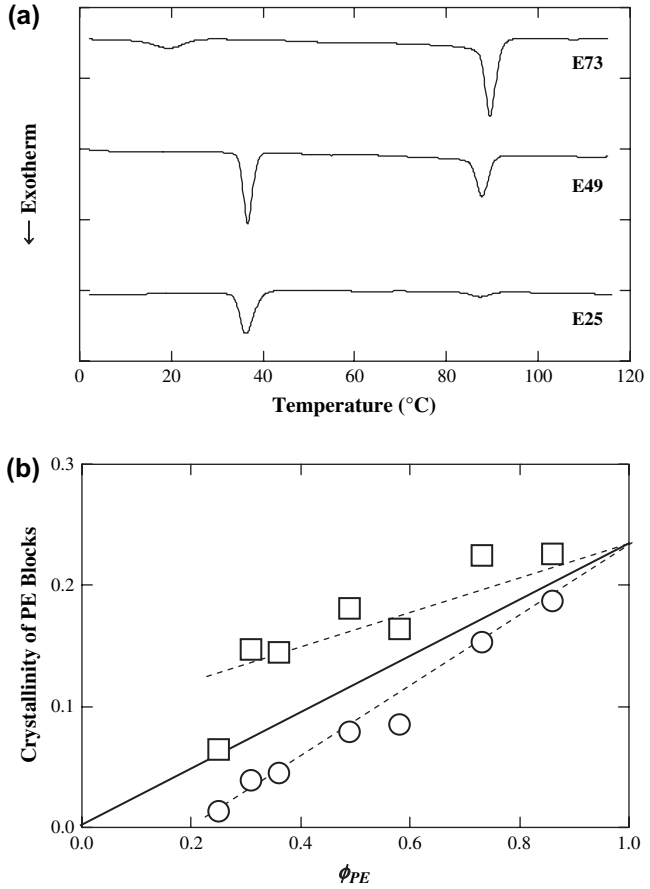

Fig. 1. (a) DSC thermograms during cooling at 10 °C/min for E73, E49, and E25. (b) The crystallinity of PE blocks in the whole sample χ_{PE} (○) and in PE blocks χ'_{PE} (□) plotted against the volume fraction of PE blocks ϕ_{PE}. The solid line represents the ϕ_{PE} dependence of χ_{PE} when we assume that the crystallization of PE blocks is not disturbed by the molten PCL.

attention on the peak position of the Lorentz-corrected SAXS curve (or long period, L) arising from the lamellar morphology formed by the crystallization of PE and/or PCL blocks. That is, we judged the morphological difference by comparing L after PCL crystallization with that of the PE lamellar morphology. This morphological difference arises virtually from the difference in the crystallization mechanism of PCL blocks at different T_cs, as we reported previously [15].

Conventional SAXS measurements were performed by using a Rigaku Nano-Viewer with a rotating-anode X-ray generator operating at 45 kV and 60 mA. The detector was a one-dimensional position-sensitive proportional counter (PSPC), and the method of data treatment was the same to that of SR-SAXS results.

3. Results and discussion

3.1. Crystallinity of PE blocks

Fig. 1a shows DSC curves during cooling at 10 °C/min for selected PCL-*b*-PE copolymers, where two exothermic peaks are observed; the peak at *ca.* 85 °C arises from the crystallization of PE blocks and that at 20–38 °C from the crystallization of PCL blocks. The exothermic peak for PCL crystallization is immature and the crystallization temperature is significantly lower for PCL-*b*-PE copolymers with a minor PCL content (E73 and also E86), suggesting that the PE lamellar morphology may be slightly different from that of other copolymers, as described in Section 2.

Fig. 1b shows the crystallinity of PE blocks in the whole system χ_{PE} (○) and in PE blocks χ'_{PE} (□) plotted against ϕ_{PE} (volume fraction of PE blocks in PCL-*b*-PE), where χ_{PE} and χ'_{PE} increase linearly with increasing ϕ_{PE} and meet at $\phi_{PE} = 1$. The small crystallinity of PE blocks at $\phi_{PE} = 1$ (*i.e.*, $\chi_{PE} = \chi'_{PE} \sim 0.24$) is due to the ethyl branch existing in PE blocks (Table 1). The moderate decrease in χ'_{PE} with decreasing ϕ_{PE} suggests that the crystallizability of PE blocks is somewhat disturbed by amorphous PCL blocks covalently connected with PE blocks; if there is no effect of amorphous PCL blocks on the PE crystallization, χ'_{PE} should be constant irrespective of ϕ_{PE}. This effect appears in the ϕ_{PE} dependence of χ_{PE}, and eventually χ_{PE} experimentally obtained is smaller than that expected without any interaction between PCL and PE blocks (solid line). Consequently, we can change χ_{PE} from 0.02 to 0.19 (and χ'_{PE} from 0.06 to 0.23) by using PCL-*b*-PE copolymers we prepared.

3.2. T_c dependence of crystallized lamellar morphology

Fig. 2 shows the SAXS curves for E73 (top), E49 (middle), and E25 (bottom) at each temperature indicated. At 130 °C, where both blocks are amorphous, a couple of scattering peaks are observed, indicating that regular microdomains are formed in the melt. By quenching each sample into low temperatures (between 20 and 45 °C), PE blocks crystallize first to form the PE lamellar morphology and subsequently PCL blocks start to crystallize from this morphology. As a result, we have various SAXS curves, in which the scattering peak is moderately diffused and the peak position depends intimately on T_c.

Fig. 3a shows the long period L of resulting morphology plotted against T_c for selected PCL-*b*-PE copolymers. For E73 (and also E86), where χ_{PE} is larger than that of other diblocks, L is constant irrespective of T_c and exactly identical with that of the morphology before PCL crystallization (which is plotted between 60 and 80 °C). On the other hand, L changes complicatedly with changing T_c for E49 and E25; for example, L for E25 at $T_c < 30$ °C is equal to that of the PE lamellar morphology (at $T_c = 60$–80 °C) while it increases further with increasing T_c up to 45 °C. This increase arises from the difference in the crystallization mechanism of PCL blocks, as we have already pointed out [14,15]; at lower T_c PCL blocks crystallize within the PE lamellar morphology to form a double crystallized alternating structure while at higher T_c they crystallize by deforming and/or partially destroying the existing PE lamellar morphology to form the PCL-based morphology.

The boundary temperature T_p between two different morphologies can be evaluated from Fig. 3a as a temperature where L deviates from that of the PE lamellar morphology

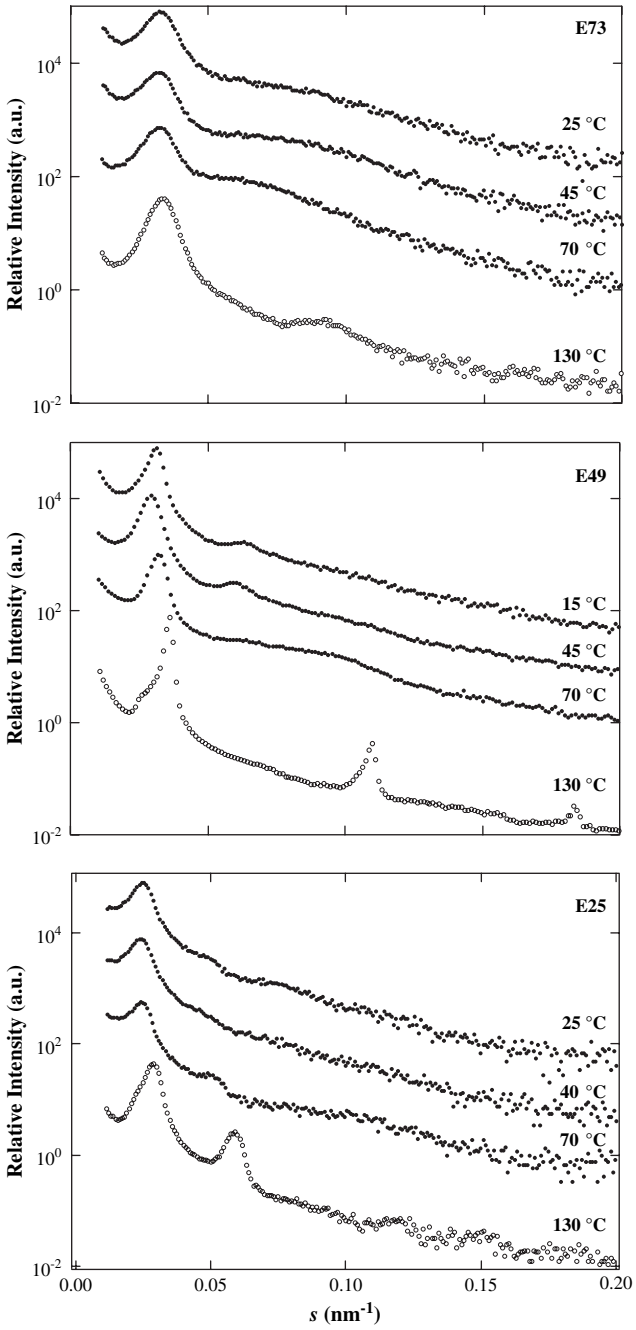

Fig. 2. SAXS intensities plotted against $s(=(2/\lambda)\sin\theta)$ for E73 (top), E49 (middle), and E25 (bottom) at each temperature indicated. Open circles represent the scattering from the molten microdomain structures.

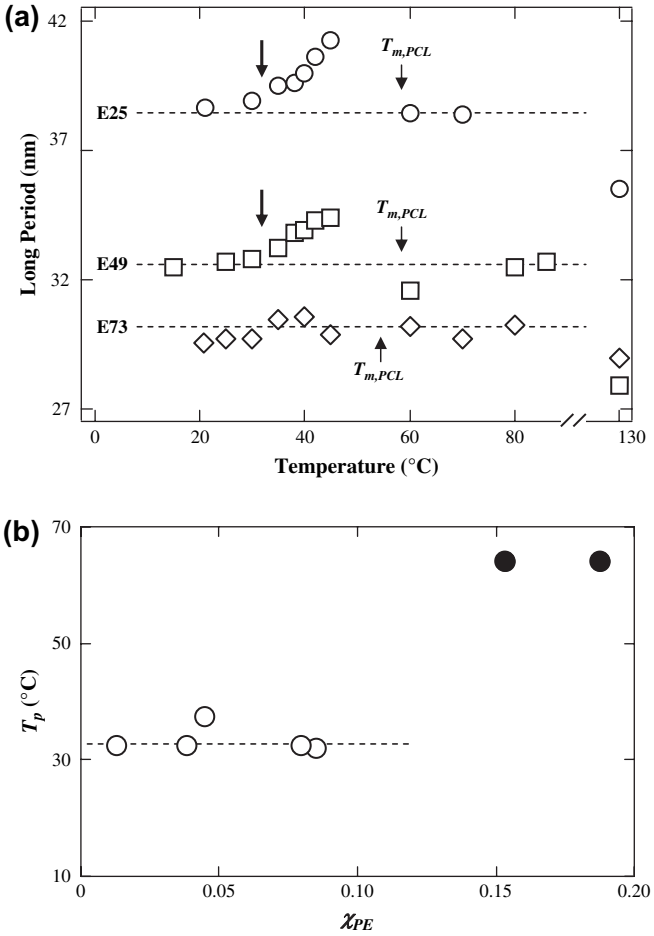

Fig. 3. (a) The long period plotted against T_c for E73, E49, and E25. (b) The boundary temperature of different morphologies T_p plotted against χ_{PE}. For E86 and E73, we could not evaluate T_p, so that we simply assumed $T_p \sim T^0_{m,PCL}$ (closed circle).

(indicated by arrows in Fig. 3a), and is plotted in Fig. 3b against χ_{PE}. We could not observe any morphological difference for E86 and E73 at every T_c investigated within our experimentally accessible time, so that we simply put $T_p \sim T^0_{m,PCL}$ in Fig. 3b, where $T^0_{m,PCL}$ is an equilibrium melting temperature of PCL homopolymer ($=64$ °C [28]). This fact indicates that the PE lamellar morphology existing in PCL-*b*-PE with $\chi_{PE} > 0.15$ effectively controls the subsequent crystallization of PCL blocks. On the other hand, T_p is almost constant ($\sim$33 °C) for PCL-*b*-PE with $\chi_{PE} < 0.10$, which arises from a competition between PCL crystallization and the confinement by the PE lamellar morphology.

3.3. Stability of PE lamellar morphology against PCL crystallization

The PE lamellar morphology consists of *hard* PE crystals and *soft* amorphous PE layers, and therefore we can expect a combination of two kinds of spatial confinement when the PCL block starts to crystallize from the PE lamellar morphology; one is the confinement usually observed in *rubbery* crystalline–amorphous diblocks [29], where the crystallization may destroy or at least deform the existing microdomain structure to yield a moderate crystallinity, and the other is that observed in *glassy* diblocks [30], where the microdomain structure cannot deform at all to have a small or no crystallinity.

Fig. 3b indicates that the confinement of the PE lamellar morphology against PCL crystallization is an intermediate between glassy and rubbery confinements. That is, when χ_{PE} is not large the PE lamellar morphology does not effectively disturb the crystallization of PCL blocks and eventually it

works as a soft confinement. Here it is easily supposed that the crystallization rate of PCL blocks, which depends significantly on T_c, controls the resulting morphology; at lower T_c, the crystallization of PCL blocks is fast enough to have no time for the morphological rearrangement, resulting in the crystallized PE lamellar morphology. At higher T_c, on the other hand, the crystallization of PCL blocks is slow, so that there is enough time for the rearrangement of the PE lamellar morphology into a new one favorable for the crystallization of PCL blocks. Therefore, T_p is substantially determined by the crystallization rate of PCL blocks and has a constant value as long as the spatial confinement by the PE lamellar morphology is not strong, that is, χ_{PE} is moderately small.

When χ_{PE} is large enough, the PE lamellar morphology acts as a hard confinement for the crystallization of PCL blocks because the solid fraction increases sufficiently in the system. In addition, the slightly different PE lamellar morphology, which was already described in Section 2, might contribute to the confinement. Consequently the PE lamellar morphology is completely preserved at every T_c and PCL blocks crystallize within it. Therefore the confined crystallization observed in PCL-*b*-PE with large χ_{PE} and that with small χ_{PE} at lower T_c arises due to different reasons. In summary, we can understand that the PE lamellar morphology works as an intermediate between rubbery and glassy confinement for the crystallization of PCL blocks, which critically depends on χ_{PE}.

Acknowledgments

This work was supported in part by NEDO (New Energy and Industrial Technology Development Organization) launched in 2001 and also by Grants-in-Aid for Scientific Research on Basic Areas (B) (No. 17350102) from the Ministry of Education, Science, Sports, and Culture of Japan. The SR-SAXS measurement has been performed under the approval of Photon Factory Advisory Committee (No. 2004G093).

References

[1] Nojima S, Ono M, Ashida T. Polym J 1992;24:1271–80.
[2] Gan Z, Jiang B, Zhang J. J Appl Polym Sci 1996;59:961–7.
[3] Floudas G, Reiter G, Lambert O, Dumas P. Macromolecules 1998;31:7279–90.
[4] Lambert O, Reutenauer S, Hurtrez G, Riess G, Dumas P. Polym Bull 1998;40:143–9.
[5] Bogdanov B, Vidts A, Schacht E, Berghmans H. Macromolecules 1999;32:726–31.
[6] Shiomi T, Imai K, Takenaka K, Takeshita H, Hayashi H, Tezuka Y. Polymer 2001;42:3233–9.
[7] Jiang S, He C, An L, Chen X, Jiang B. Macromol Chem Phys 2004;205:2229–34.
[8] Sun J, Chen X, He C, Jing X. Macromolecules 2006;39:3717–9.
[9] Ueda M, Sakurai K, Okamoto S, Lohse DJ, MacKnight WJ, Shinkai S, et al. Polymer 2003;44:6995–7005.
[10] Albuerne J, Marquez L, Muller AJ, Raquez JM, Degee PH, Dubois PH, et al. Macromolecules 2003;36:1633–44.
[11] Ho RM, Hsieh PY, Tseng WH, Lin CC, Huang BH, Lotz B. Macromolecules 2003;36:9085–92.
[12] Maglio G, Migliozzi A, Palumbo R. Polymer 2003;44:369–75.
[13] Balsamo V, Gil G, Navarro CU, Hamley IW, Gyldenfeldt F, Abetz V, et al. Macromolecules 2003;36:4515–25.
[14] Nojima S, Akutsu Y, Washino A, Tanimoto S. Polymer 2004;45:7317–24.
[15] Nojima S, Akutsu Y, Akaba M, Tanimoto S. Polymer 2005;46:4060–7.
[16] Hamley IW, Castelletto V, Castillo RV, Muller AJ, Martin CM, Pollet E, et al. Macromolecules 2005;38:463–72.
[17] Radano CP, Scherman OA, Stutzmann NS, Muller C, Breiby DW, Smith P, et al. J Am Chem Soc 2005;127:12502–3.
[18] Hamley IW, Parras P, Castelletto V, Castillo RV, Muller AJ, Pollet E, et al. Macromol Chem Phys 2006;207:941–53.
[19] Yang J, Zhao T, Cui J, Liu L, Zhou Y, Li G, et al. J Polym Sci Part B Polym Phys 2006;44:3215–26.
[20] Hamley IW. The physics of block copolymers. Oxford: Oxford University Press; 1998.
[21] Hamley IW. Adv Polym Sci 1999;148:113–37.
[22] Loo YL, Register RA. In: Hamley IW, editor. Developments in block copolymer science and technology. New York: Wiley; 2004.
[23] Muller AJ, Balsamo V, Arnal ML. Adv Polym Sci 2005;190:1–63.
[24] Nojima S, Kato K, Yamamoto S, Ashida T. Macromolecules 1992;25:2237–42.
[25] Quiram DJ, Register RA, Marchand G. Macromolecules 1997;30:4551–8.
[26] Brandrup J, Immergut EH, editors. Polymer handbook. 3rd ed. New York: Wiley; 1989.
[27] Nojima S, Kikuchi N, Rohadi A, Tanimoto S, Sasaki S. Macromolecules 1999;32:3727–34.
[28] Chatani Y, Okita Y, Tadokoro H, Yamashita Y. Polym J 1970;1:555–62.
[29] Nojima S, Hashizume K, Rohadi A, Sasaki S. Polymer 1997;38:2711–8.
[30] Nojima S, Tanaka H, Rohadi A, Sasaki S. Polymer 1998;39:1727–34.